CHEMISTRY OF MATERIALS

Article

pubs.acs.org/cm

Mechanical Properties of a Library of Low-Band-Gap Polymers

Bérenger Roth,[†,‡] Suchol Savagatrup,[§,‡] Nathaniel V. de los Santos,[§] Ole Hagemann,[†] Jon E. Carlé,[†] Martin Helgesen,[†] Francesco Livi,[†] Eva Bundgaard,[†] Roar R. Søndergaard,[†] Frederik C. Krebs,[†] and Darren J. Lipomi*[,§]

[†]Department of Energy Conversion and Storage, Technical University of Denmark, Frederiksborgvej 399, DK-4000 Roskilde, Denmark

[§]Department of NanoEngineering, University of California San Diego, 9500 Gilman Drive, Mail Code 0448, La Jolla, California 92093−0448, United States

Supporting Information

ABSTRACT: The mechanical properties of low-band-gap polymers are important for the long-term survivability of roll-to-roll processed organic electronic devices. Such devices, e.g., solar cells, displays, and thin-film transistors, must survive the rigors of roll-to-roll coating and also thermal and mechanical forces in the outdoor environment and in stretchable and ultraflexible form factors. This paper measures the stiffness (tensile modulus), ductility (crack-onset strain), or both of a combinatorial library of 51 low-band-gap polymers. The purpose of this study is to systematically screen a library of low-band-gap polymers to better understand the connection between molecular structures and mechanical properties in order to design conjugated polymers that permit mechanical robustness and even extreme deformability. While one of the principal conclusions of these experiments is that the structure of an isolated molecule only partially determines the mechanical properties—another important codeterminant is the packing structure—some general trends can be identified. (1) Fused rings tend to increase the modulus and decrease the ductility. (2) Branched side chains have the opposite effect. Despite the rigidity of the molecular structure, the most deformable films can be surprisingly compliant (modulus ≥ 150 MPa) and ductile (crack-onset strain ≤ 68%). This paper concludes by proposing a new composite merit factor that combines the power conversion efficiency in a fully solution processed device obtained via roll and roll-to-roll coating and printing (as measured in an earlier paper) and the mechanical deformability toward the goal of producing modules that are both efficient and mechanically stable.

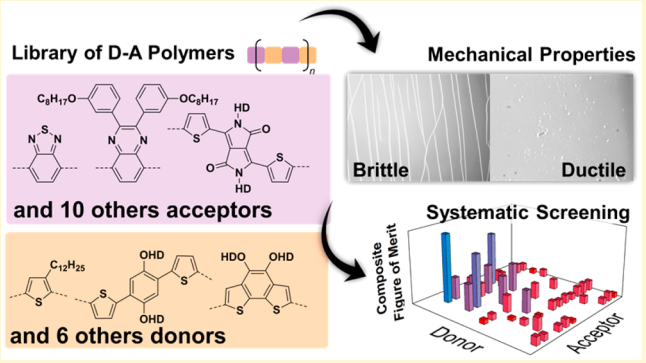

INTRODUCTION

The conventional rationale for research on organic photovoltaic (OPV) materials and devices is the promise of inexpensive, lightweight, flexible solar modules that can be fabricated by roll-to-roll (R2R) processing in ambient atmosphere on flexible substrates.[1] These defining advantages are thus contingent on stability against bending and other thermomechanical modes of deformation.[2] The work of Dauskardt et al. has shown, however, that the cohesive and adhesive fracture energies encountered within and between layers in organic solar cells occupy a typical range of 1−5 J m^{-2}, which is significantly lower than the values that characterize devices based on conventional semiconducting materials (though these values are dependent on the thickness of the active layer, polymer:fullerene blend, processing conditions, composition, molecular weight, and relative humidity).[3] Despite an increase in interest in the mechanical properties of nominally flexible electronic materials,[4,5] almost all previous work has focused on the properties of poly(3-alkylthiophenes) (P3ATs, for which we have previously shown that structural features such as the length of the alkyl side chain play critical roles in determining the stiffness, yield point, and ductility of conjugated polymers[2,6]). While the P3ATs (particularly where A = hexyl) have been a useful model system,[7] and also appears to have significant advantages in R2R production,[8] the best power conversion efficiencies are achieved with low-band-gap polymers comprising an alternating arrangement of donor and acceptor (D−A) units.[9]

This paper describes a large-scale investigation of the mechanical properties of D−A polymers by measuring the tensile modulus, cracking behavior, or both of a combinatorial library of 51 compounds, which represent combinations of acceptors A1−10 and A12−14 and donors D1−D3 and D5−D9, shown in Figure 1. The purpose of this study was to take the first steps toward developing guidelines for the rational design of conjugated polymers for increased mechanical stability and deformability. Combined with an earlier report

Received: February 4, 2016
Revised: March 14, 2016
Published: March 14, 2016

DOI: 10.1021/acs.chemmater.6b00525
Chem. Mater. 2016, 28, 2363−2373

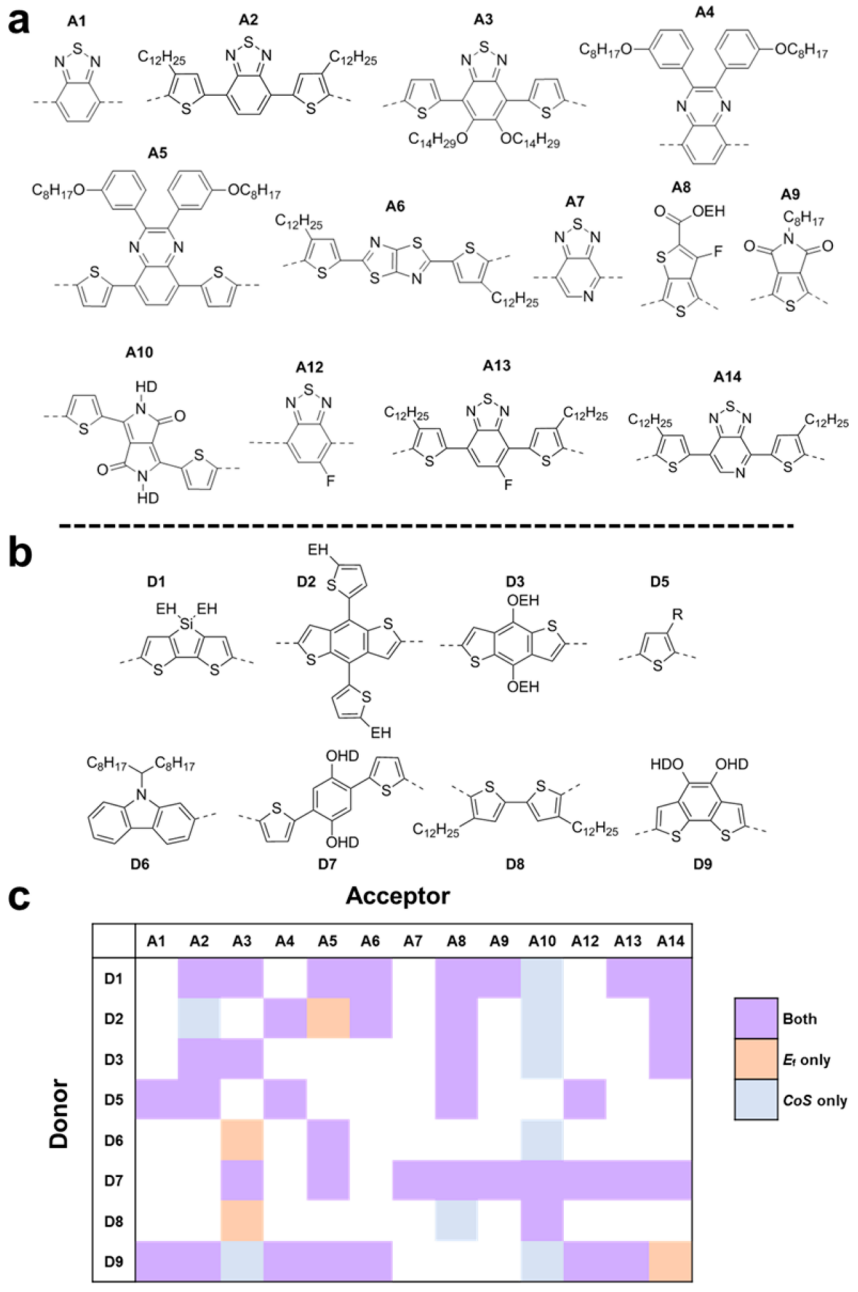

Figure 1. Chemical structures of the 13 acceptor monomers (a) and 8 donor monomers (b) as synthesized and described in a previous paper.[8] (c) Table of the combination of D−A polymers measured in this work. Tensile moduli (E_f) were measured for a total of 43 polymers, the crack-onset strains (*CoS*) were measured for 47 polymers, and both quantities were measured for 39 polymers. The "missing" combinations are the result of failure to obtain the material by synthesis, failure to create devices via roll coating, or insufficient material available after the initial studies performed in ref 8. For D5, R is H for A2 and A4 and $C_{12}H_{25}$ for A1, A8, and A12. The abbreviation EH stands for 2-ethylhexyl, and HD stands for 2-hexyldecyl.

from Bundgaard et al.[8] on the photovoltaic performance of a library of which the materials studied here is a subset, the ultimate goal of this work is thus to permit the co-optimization of electronic and mechanical performance. A favorable outcome would not only improve the stability of R2R-processed organic solar modules but also allow the integration of OPVs—or any organic electronic devices—in many form factors inaccessible by conventional devices, such as in clothing, portable electronics, biomedical applications, and extremely flexible and stretchable devices.[2]

BACKGROUND

The mechanical stability of conjugated polymers, specifically D−A polymers, has until now received little attention in the literature. The absence of emphasis on this topic has been due to the focus on improving the power conversion efficiency (*PCE*) on a small-scale laboratory device on glass where thermomechanical properties rarely present a limitation to observations of device performance. However, for flexible devices that require flexibility during manufacturing, in the actual application/integration, and in the operation of the device, the thermomechanical properties become a dominant boundary condition that if not met will prevent success

DOI: 10.1021/acs.chemmater.6b00525
Chem. Mater. 2016, 28, 2363−2373

(regardless of device *PCE*).[1] Recently, laboratory-scale *PCE* for D−A polymers has reached well over 10% on optimized architectures on devices with small active areas.[10] However, these devices were prepared on rigid substrates, i.e., glass coated with indium tin oxide (ITO), that are not compatible with R2R manufacturing.[1] Moreover, rigid substrates mask the potential fragility of the D−A polymers and polymer:fullerene composites that could lead to mechanical failure in flexible modules.[2] The recent effort by Bundgaard et al. to screen 104 different combinations of D−A polymers has revealed that 13 out of 104 polymers outperformed P3HT on a merit factor that is weighted toward the suitability of the materials for R2R processing.[8] This merit factor accounted for not only the electrical performance but also the chemical stability and simplicity of the synthesis[8] but did not account for the predicted stability against thermomechanical degradation.

While most earlier work by us and others on the mechanical properties of organic semiconductors has focused on P3ATs,[2] a few studies have suggested some ways in which the molecular structures of the D−A polymers influence their mechanical properties. An earlier paper examined the mechanical properties of PDPP-2TTT (a D−A polymer whose repeating units comprise diketopyrrolopyrrole (DPP), thiophene (T), thienothiophene (TT), and thiophene in the backbone) and PDPP-4T (a close structural analog in which the fused thienothiophene structure was substituted with bithiophene, which comprises two isolated thiophene rings).[11] The results of this work suggested (though not rigorously confirmed) that the polymer with the fused ring system produced a tensile modulus that was higher (0.99 GPa for PDPP-2TTT) than that of the polymer bearing the isolated rings (0.74 GPa for PDPP-4T).[11] In a separate study, we found that random incorporation of bithiophene units into the structure of PDPP-2FT (where F = furan) decreased the tensile modulus from 2.17 ± 0.35 to 0.93 ± 0.16 GPa.[12] The brittleness of polymers comprising rigid large fused rings in the backbone was also suggested by the results of Wu et al., who observed significant cracking in highly crystalline organic thin film transistors fabricated from a DPP-based polymer with four fused thiophene rings.[13] Additionally, Kim et al. also investigated the mechanical properties of D−A polymers, namely, that of PBDTTTPD (same structure as A9D2, however we did not have this material available for this study).[14] They found that the tensile modulus of the composite of PBDTTTPD and a nonfullerene electron acceptor (at 1:1 ratio) was 0.43 GPa, which is much lower than when combined with PCBM at 1.76 GPa (at 1:1.5 ratio), and were able to make a solar cell with good efficiency and high intrinsic deformability.[14] These experimental results have recently been complemented with computational tools designed to study the effects of molecular structures of conjugated polymers on mesoscale (∼10−100 nm) conformational structures and thus may also accelerate the understanding of the connection between molecular structure and mechanical properties.[15]

Despite the efforts noted above, mechanical data for D−A polymers is sparsely reported. We thus sought to lay the groundwork for a rigorous understanding of the structural determinants of the mechanical properties of D−A polymers by reporting the properties of a sufficiently large library comprising several popular donors and acceptors. We admit at the outset several limitations of this approach. First, the mechanical properties of polymers are determined not only by the molecular structure but also by the microstructure in the solid state. The microstructure/morphology is difficult to predict by computation[15] (though eventually it should be possible to do so), and moreover, the microstructure/morphology was not within our means to measure for the entire library. Second, the microstructure/morphology that forms is a strong function of the solvent, film-casting method, drying, and postprocessing steps,[9,16] which it was not practical to optimize for every material. Third, the molecular weight and dispersity ($Đ$) for step-growth polymerizations are notoriously difficult to control, though it is possible that the stiffness of D−A polymers precludes a highly entangled microstructure, even at high molecular weights.[17] Fourth, the mechanical properties of bulk heterojunction films are significantly affected by the electron-transporting phase.[2] For polythiophenes, we found that the tensile moduli of polythiophene:[60]PCBM blends was linearly correlated to the tensile moduli of the pure polymers,[18] though this behavior cannot be assumed for all polymers nor can it be assumed that methanofullerenes will be used in all organic solar cells in the future, and thus, we measured the properties of the pure polymers only. Despite these limitations, we found that several rules of thumb did emerge for increased deformability of D−A polymers. Moreover, we expect that the mechanical characteristics of the library of polymers reported here will stimulate computational and microstructural studies designed to connect molecular structure not only to electronic performance but also to mechanical behavior.

EXPERIMENTAL DESIGN

Selection of Materials. We selected the combination of 8 different donor monomers and 13 different acceptor monomers in order to test a library of D−A polymers with diversity in chemical structures (Figure 1a and 1b). The library is a subset of that used in a recent paper by Bundgaard et al. on the viability of these materials for R2R fabrication.[8] The chemical structures were selected on the basis of polymers from the current literature that produced highly efficient solar cells, including polymers containing the subunits benzothiadiazole (BT), quinoxaline (as seen in TQ1), benzodithiophene (BDT), diketopyrrolopyrrole (DPP), carbozole, thiophene, and bithiophene. Our initial hypothesis was that two prominent features of the chemical structures—(1) fused vs isolated rings and (2) branched vs linear side chains—would affect the mechanical properties of the films bearing them. The monomers containing fused rings are A6, A10, D1, D2, D3, D6, and D9. We made the distinction between structures with fused rings aligned along the backbone such as those found in diketopyrrolopyrrole (DPP) and fused rings not in the direction of the backbone such as benzothiadiazole (BT). The solubilizing side chains on the structures range from relatively short alkyl side chains of eight carbons (C_8H_{17}) to long alkyl side chains of 14 carbons ($C_{14}H_{29}$) as well as branching side chains of 2-ethylhexyl (EH) and 2-hexyldecyl (HD). We also examined the effects of molecular weight and dispersity on the mechanical properties of the polymers.

Measurement of Mechanical Properties. We measured the mechanical properties of the D−A polymers using two specific values: tensile modulus and the crack-onset strain. Both measurements are performed using the film-on-elastomer techniques. In particular, the tensile moduli were measured using the buckling instability as developed by Stafford et al.,[19] expanded to conjugated polymers by Tahk et al.,[20] and used extensively by us and others.[2,4,11,21] Low tensile modulus is regarded as "good" from the standpoint of mechanical stability,

DOI: 10.1021/acs.chemmater.6b00525
Chem. Mater. 2016, 28, 2363−2373

because films that require a low energy density to elongate in the elastic regime will minimize interfacial stresses with other layers in the device stack that would otherwise lead to delamination.[2,22] For polythiophenes of comparable molecular weight, low tensile modulus is also highly correlated to high crack-onset strain. Crack-onset strains of films on elastomers are often interpreted as analogous to the elongation at fracture of bulk samples or free-standing films of the polymers, though these quantities are not exactly equivalent because poor adhesion of a film to a substrate—and unequal adhesion among different polymers—localizes strain to cracks and defects and causes premature cracking.[4,23] The polymer films were transferred to elastomeric substrates and stretched, and we recorded the crack onset strain by obtaining micrographs at each level of strain. We also took note of the qualitative nature of the cracks, i.e. either brittle cracks (which propagated the entire length of the film perpendicular to the stretched axis) or ductile cracks (whose propagation was limited). We note that previous studies by Stafford and co-workers[19,24,25] and O'Connor et al.[4] have shown that the tensile modulus of a thin film is a relatively weak function of its thickness when the film is above ∼40 nm and below 500 nm. We judiciously prepared our thin films to be within this range. We also observed no significant deviation from the averaged value of the crack-onset strain for any polymer sample. Furthermore, we chose this range of film thicknesses to better correlate with the result from Bundgaard et al., in which the thicknesses of all devices were between 300 and 500 nm.[8]

RESULTS AND DISCUSSION

Tensile Moduli of Low-Band-Gap D−A Polymers. We began by measuring the tensile modulus of each D−A polymer using the buckling-based method. Figure 2a shows a comprehensive overview of all tensile moduli collected for the available polymers. The standard deviation of each value was calculated from the propagation of standard errors of the line fits (buckling wavelength vs film thickness) and the standard deviation of the tensile moduli of the PDMS substrates; the values are provided in Table 1. We discarded the values of the modulus from the samples in which the standard errors of the line fits were too high ($R^2 < 0.95$) or the characteristic buckling wavelengths could not be obtained. The reasons for the failure to obtain good linear fits or a consistent buckling wavelength arose from the difficulty in handling some thin films. In some cases, the films adhered too well to the glass substrates; strong adhesion to the glass substrate led to either partial transfer onto the PDMS substrate or damage to the films. For other cases, the strain induced by handling the transferred film on PDMS or the compressive strain induced to generate buckles resulted in delamination or cracking of the films or both. These defects in the films resulted in the misrepresentation of the buckling wavelengths because the compressive strain was accommodated by delamination and cracking, as opposed to by buckling.[26] Polymers with a high tendency to crack under the minute strains produced by transfer were treated as having effective crack-onset strains of 0%. Measurements of the crack-onset strain, described in the next section, were performed to further test the dependency of ductility on molecular structure.

The values of the tensile modulus occupied a range between 200 MPa and 4 GPa, which corresponded well with the range of the previously reported moduli for other D−A conjugated polymers using the same method of measurement.[2] The highest

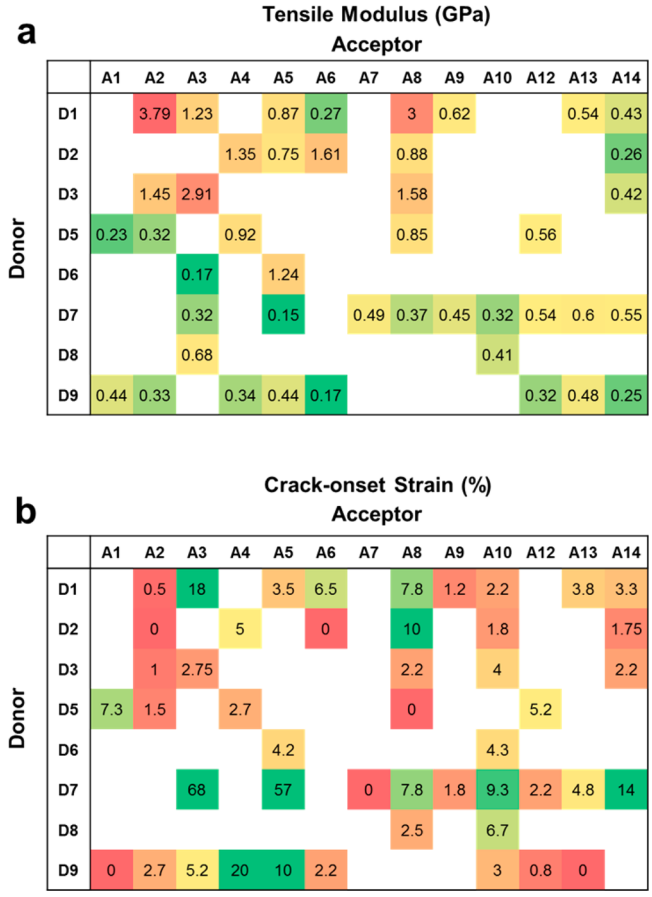

Figure 2. Summary of the mechanical properties measured in this paper. (a) Tensile moduli of the examined polymers in GPa. Indicated colors correspond to the ranking of the lowest value of the modulus (green) to the highest value of the modulus (red). (b) Crack-onset strain of the polymers. Colors correspond to the ranking from the highest value (green) to the lowest value (red). Standard deviations are omitted in this figure for the sake of clarity and provided in Table 1. No values were plotted for the polymers for which the measurements were not obtained.

value of tensile modulus measured was that of A2D1 at 3.79 ± 0.80 GPa. The first qualitative trend we observed was the relatively high stiffness (larger values of tensile moduli) of polymers comprising donor units with fused rings in the backbone. The polymers with donor units with fused rings (D1, D2, and D3) were found to have an average tensile modulus on the order of 1 GPa, while polymers with isolated rings such as D5, D7, and D8 had moduli on the order of 500 MPa. This qualitative trend agrees well with the previously reported increase in stiffness when the polymer backbone comprises fused rings rather than isolated rings.[11] We note here that D6 and D9 also comprise fused rings in their backbone; however, the resulting polymers from these two donor units were found to have much lower average modulus, which was similar to values obtained for polymers with isolated rings. We attributed this lower than expected moduli to the presence of long and branched solubilizing side chains found on both D6 and D9.

The effect of the length of the solubilizing side chains on the tensile modulus of P3AT was studied by us in a previous publication.[23] We found that an increase in the length of the alkyl side chain from 4 to 8 (P3BT to P3OT) dramatically reduced the tensile modulus by approximately an order of magnitude. This effect was attributed to the decrease in glass

DOI: 10.1021/acs.chemmater.6b00525
Chem. Mater. 2016, 28, 2363−2373

Table 1. Tensile Moduli and Crack-Onset Strain of All Polymers Measured by the Film-on-Elastomer Technique in This Study[a]

polymer	M_n (Da)	$Đ$	tensile modulus (GPa)	crack-onset strain (%)	crack behavior
A1D5	9300	2.2	0.24 ± 0.08	7.3 ± 2	ductile
A1D9	6900	1.4	0.44 ± 0.18	0[c]	brittle
A2D1	9500	2.0	3.79 ± 0.80	0.5[d]	brittle
A2D2	12 400	11.4	NA[b]	0[c]	brittle
A2D3	90 000	4.5	1.45 ± 0.47	1[d]	brittle
A2D5	540 000	4.2	0.32 ± 0.02	1.5[d]	brittle
A2D9	9400	1.8	0.33 ± 0.12	2.7 ± 1.5	brittle
A3D1	50 000	10.8	1.23 ± 0.52	18 ± 5	ductile
A3D3	16 000	3.5	2.91 ± 1.30	2.75[d]	brittle
A3D6	3800	3.1	0.17 ± 0.02	NA[b]	NA
A3D7	24 000	2.7	0.32 ± 0.03	68 ± 14	ductile
A3D8	2200	3.1	0.68 ± 0.14	NA[b]	NA
A3D9	19 000	2.1	NA[b]	5.2 ± 2	ductile
A4D2	22 000	9.1	1.35 ± 0.76	5.0 ± 1.3	brittle
A4D5	29 000	9.2	0.92 ± 0.19	2.7 ± 0.6	brittle
A4D9	7000	1.5	0.34 ± 0.18	19.7 ± 1.5	ductile
A5D1	18 000	3.0	0.87 ± 0.11	3.5 ± 0.5	brittle
A5D2	100 700	3.1	0.75 ± 0.23	NA[b]	NA
A5D6	11 000	26.7	1.24 ± 0.29	4.2 ± 1.3	brittle
A5D7	34 000	3.4	0.15 ± 0.04	56.8 ± 9.9	ductile
A5D9	138 000	8.0	0.44 ± 0.15	10 ± 3.6	ductile
A6D1	9600	2.0	0.27 ± 0.02	6.5 ± 2.0	brittle
A6D2	11 000	2.2	1.61 ± 0.51	0[c]	brittle
A6D9	21 600	2.7	0.17 ± 0.05	2.2 ± 0.8	brittle
A7D7	1200	3.3	0.49 ± 0.18	0[c]	brittle
A8D1	16 000	2.0	3.00 ± 0.56	7.8 ± 0.8	brittle
A8D2	14 000	2.4	0.88 ± 0.40	10 ± 2	ductile
A8D3	14 000	2.2	1.58 ± 0.64	2.2 ± 0.8	brittle
A8D5	5000	1.4	0.85 ± 0.21	0[c]	brittle
A8D7	6100	2.6	0.37 ± 0.10	7.8 ± 1.6	ductile
A8D8	3700	2.2	NA[b]	2.5 ± 1.5	brittle
A9D1	9500	2.8	0.62 ± 0.20	1.2 ± 0.6	brittle
A9D7	7200	1.7	0.45 ± 0.17	1.8 ± 0.3	brittle
A10D1	21 000	2.5	NA[b]	2.2 ± 0.8	brittle
A10D2	103 000	3.3	NA[b]	1.8 ± 0.6	brittle
A10D3	68 000	3.3	NA[b]	4 ± 1	brittle
A10D6	6700	3.5	NA[b]	4.3 ± 1.3	brittle
A10D7	34 000	4.2	0.32 ± 0.06	9.3 ± 1.5	ductile
A10D8	1200	2.8	0.41 ± 0.22	6.7 ± 0.8	ductile
A10D9	2300	5.4	NA[b]	3 ± 1.7	brittle
A12D5	13 000	3.1	0.56 ± 0.25	5.2 ± 2.4	brittle
A12D7	5600	2.1	0.54 ± 0.24	2.2 ± 0.8	brittle
A12D9	37 000	2.3	0.32 ± 0.05	0.8 ± 0.6	brittle
A13D1	12 000	7.5	0.54 ± 0.25	3.8 ± 2.4	brittle
A13D7	10 000	2.1	0.60 ± 0.16	4.8 ± 0.3	brittle
A13D9	12 000	76.7	0.48 ± 0.13	0[c]	brittle
A14D1	9800	1.7	0.43 ± 0.26	3.3 ± 0.8	brittle
A14D2	4600	4.1	0.26 ± 0.05	1.75[d]	brittle
A14D3			0.42 ± 0.14	2.2 ± 1.0	brittle
A14D7	19 000	2.6	0.55 ± 0.09	13.7 ± 1.5	ductile
A14D9	1600	1.9	0.25 ± 0.12	NA[b]	NA

[a]The number averaged molecular weights and the values of dispersity are reproduced from ref 8. Polymers are separated by the designated number of the acceptor (Figure 1) for readability. [b]The values obtained from so-designated polymer samples were omitted or removed due to (1) insufficient material available, (2) failure to obtain smooth films, or (3) too large of propagated error. [c]The polymer samples cracked upon the start of the test under the strain of less than the minimum step of 0.5% strain. [d]The polymer samples exhibited inconsistent cracking behaviors, and the values of the crack-onset strains reported are the lowest measured crack-onset strains.

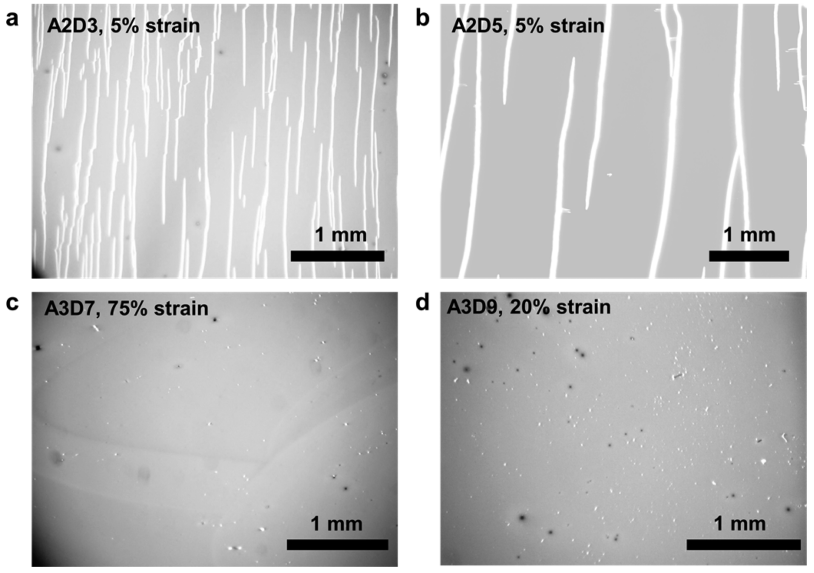

Figure 3. Optical micrographs of the two different natures of cracking behavior: brittle fracture (a, b) and ductile fracture (c, d).

transition temperature with longer side chains and the reduction of the volume fraction of the load-bearing main chain.[23] The presence of the long and branching side chains have been known to affect the microstructure and therefore electronic properties of the polymers in many aspects, for example, by increasing the separation between main chains.[16] This reduction in the intermolecular packing of the polymer

DOI: 10.1021/acs.chemmater.6b00525
Chem. Mater. 2016, 28, 2363−2373

chains could explain the large reduction in tensile moduli found in polymers comprising D6 and D9.

Ductility of D−A Polymers. We measured the ductility of the D−A polymers as manifested in the crack-onset strain.[4,11,23] Figure 2b shows the average values of the crack-onset strains. The standard deviations, reported in Table 1, were taken from the statistics from measurements of different samples ($N > 3$). Six polymers cracked upon preparation of the film, transferring onto an elastomer substrate and mounting the film-on-elastomer onto the linear actuator, and their values are reported as 0% strains in Figure 2b and Table 1. However, it is important to note that despite the effort to minimize the applied strain during preparation of the samples, some finite tensile strains were induced during the preparation stages. We estimated this value to be lower than 0.5%.

We found that the majority of D−A polymers has relatively low crack-onset strains when compared to other conjugated polymers such as P3ATs. Most of the D−A polymer films experienced catastrophic cracking at tensile strains lower than 5% (Figure 2b). The cracking behavior of each film is also summarized in Table 1. We observed that the films with crack-onset strains below 5% cracked in a brittle mode. Specifically, the cracks that formed in these films tended to propagate rapidly along the entire axis perpendicular to the strained axis. In contrast, a few polymers comprising the combination of monomers A3, A8, D1, D5, D7, and D9 were found to have higher crack-onset strains (highlighted in green in Figure 2b). The increased crack-onset strains for these polymer films could potentially be explained by the nature of the ductile fracture found in these films. Cracks found in these polymer films, labeled "ductile" in Table 1, appeared as pinholes and exhibited less of a tendency to propagate with increased strain (qualitatively equivalent to greater fracture toughness). The example of the visual contrast between the two cracking behaviors is shown in Figure 3. While both brittle and ductile fractures are deleterious to the films and possibly to the performance of a fully fabricated OPV, the ductile films would have a lower tendency to propagate cracks and to cause failure, i.e., short circuits in devices with vertical charge transport (solar cells) and open circuits in devices requiring horizontal charge transport (thin-film transistors).

Previous studies on conjugated polymers have found a correlation between tensile modulus and the propensity of the polymer films to crack upon the applied tensile strains, i.e., films with higher moduli tend to crack at lower applied strains. However, these studies are usually performed on P3ATs.[21,23] The same correlation was not found when comparing the D−A polymers of vastly different structures. Figure 4 shows the crack-onset strain as a function of tensile modulus of 39 polymers (the subset of the library for which we were able to measure both tensile modulus and crack-onset strain). As described earlier, most of the samples with higher crack-onset strain exhibited ductile fractures (blue), and those with lower values exhibited brittle fractures (red). For many polymers, despite the low values of stiffness, the films did not appear to be ductile as previously predicted for P3ATs. From the 47 polymers in which the crack-onset strains were measured, only 16 polymers withstood at least 5% tensile strains before fracture. The brittleness of D−A polymers has also been reported in mixtures with either [60] PCBM or non-PCBM electron acceptor. Kim et al. measured the mechanical properties via the pseudo-free-standing tensile test for composite of PBDTTTPD (A9D2) and PCBM or P-

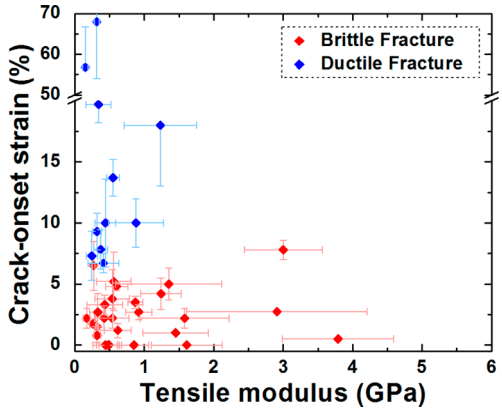

Figure 4. Plot of crack-onset strains vs tensile moduli of the polymers tested in this study. Data points are distinguished in color by the nature of the fracture: red (brittle) and blue (ductile).

(NDI2HD-T), a non-PCBM electron acceptor, by obtaining a pull test of the film supported on the surface of water.[14] The authors reported that the mixtures with PCBM cracked well before 0.30% strain, and the mixture with P(NDI2HD-T) cracked around 7% strain.[14] This apparent brittleness was further elucidated in the comparison between P3HT and PTDPPTFT4 (a DPP-based polymer with a ladder-like unit in the backbone comprising four fused thiophene rings) by Wu et al.;[13] P3HT films fabricated in the same manner as the D−A polymer could withstand over 100% tensile stains in contrast to <5% for the D−A polymer. Despite the lack of the inverse correlation between the stiffness and ductility of the D−A polymers, both quantities will be important for the implementation of a full working device designed for R2R fabrication.

Toward Rational Design for Mechanical Deformability. We sought to identify the molecular structural determinants that influence the mechanical properties of D−A polymers in an effort to co-optimize the mechanical and electrical performance and scalability, and found some general trends which could lead to qualitative design rules. However, exceptions to the rules were also identified. These exceptions could potentially arise from the indirect comparison between the combinations of donor and acceptor and the differences in molecular weight, dispersity, and possibly effects of certain combinations of donor and acceptor monomers that are otherwise difficult to predict. Critically, predictive trends in mechanical properties require understanding both the molecular structure and the solid-state microstructure or the way that the former produces the latter.[2] Solid-state packing structures[4] have been shown to greatly influence the mechanical properties, and certain combinations of monomers may lead to vastly different packing structures than those with similar donor or acceptor monomers.[12] For example, Mei et al. studied the effect of the addition of aliphatic conjugation-break spacers into the conjugated backbone of DPP-based polymers.[27] While the lamella spacing as measured from grazing incidence X-ray diffraction (GIXRD) decreased monotonically with higher concentration of the aliphatic conjugation-break spacers, the order of the crystalline domains, manifested as the lamella peak full width at half-maximum (fwhm), followed a nonlinear progression.[27] This result illustrated the competition between multiple effects of the molecular structures of the polymer: while the addition of conjugation-break spacers increased the

DOI: 10.1021/acs.chemmater.6b00525
Chem. Mater. 2016, 28, 2363−2373

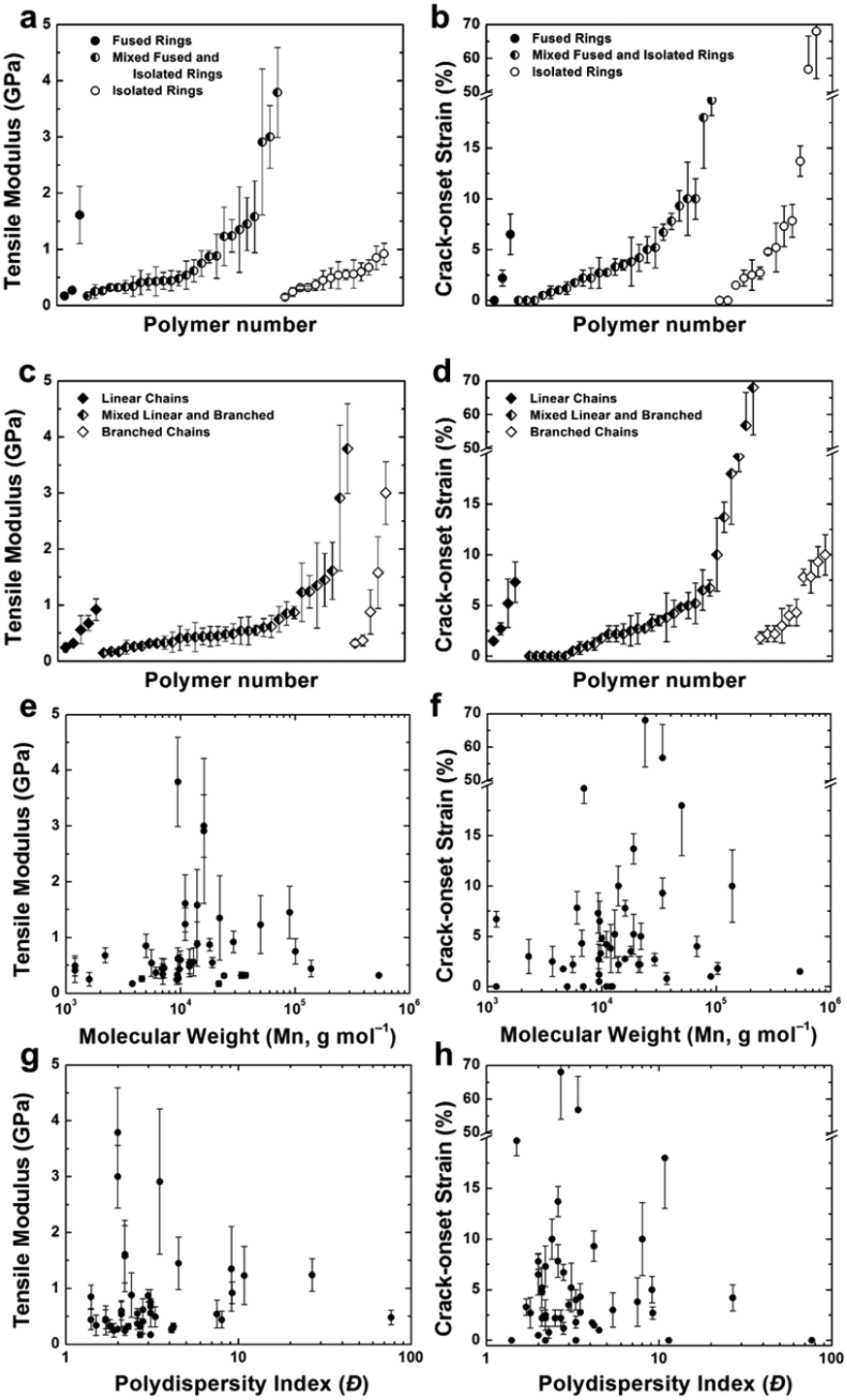

Figure 5. Illustration of the range of tensile modulus and crack-onset strains from all polymer samples. (a, b) Ranking of the polymer samples separated by the presence of fused rings in both donor and acceptor (filled circles), either fused ring in donor or acceptor (half-filled circles), and all isolated rings (open circles). (c, d) Plot in which the polymer samples are separated by the nature of the solubilizing side chains: all linear chains (filled diamonds), branched chain on either the donor or the acceptor monomers (half-filled diamonds), and all branched side chains (open diamonds). Plots of tensile moduli and crack-onset strains as a function of number-average molecular weight (e and f) and $Đ$ (g and h); values of M_n and $Đ$ are reproduced from ref 8.

flexibility of the backbone, it also increased the tendency of interdigitation of the alkyl side chains.[27] We outlined these trends in molecular structures below along with the identified exceptions.

1. Presence of Fused Rings in the Backbone. We found that the polymers with fused rings in the backbone structures (namely, the polymers with D1, D2, and D3) had average tensile moduli on the order of 1 GPa. This value is of the same order as that of regioregular P3HT.[20,23] We attributed the increase in tensile moduli for these polymers to the fact that a fused ring reduces the flexibility while increasing the length of conjugation of the backbone. Polymers with donors comprising isolated rings (D5, D7, and D8) also showed an averaged tensile modulus of 0.58, 0.42, and 0.55 GPa with the highest

DOI: 10.1021/acs.chemmater.6b00525
Chem. Mater. 2016, 28, 2363−2373

values coming from A4D5 (0.92 ± 0.19). There are, however, exceptions to this general trend, namely, the polymers comprising the donor unit D9 were found to have much lower tensile moduli, on the order of 500 MPa. This reduction in modulus for the D9 monomer was likely the effect of long and branching solubilizing side chains (2-hexyldecyl), which is further discussed in the next section. We found small effects on the tensile modulus from acceptors with fused-ring structures (A6 and A10). In addition, the polymer A6D1 that contained fused ring structures in both the donor and the acceptor monomers has a tensile modulus of only 0.27 ± 0.02 GPa.

The effects of fused rings on ductility were found to be less obvious. The values of the crack-onset strains of polymers containing D3 were found to be low (<5% crack-onset strain) and consistent with the trend, in which the fused ring in the backbone produced brittle polymer films. However, for polymers comprising D1 and D2, some combinations with certain acceptor monomers were found to produce ductile films, namely, A3D1 and A8D2 exhibited ductile fractures with crack-onset strain higher than 10%. Again, we believed the abnormality in the trend was the product of the side chains on the acceptors, which will also be discussed in the next section. The polymers containing the fused DPP monomer (A10) when combined with donor monomer with fused rings (D1, D2, D3, D6, and D9) also produced brittle films (i.e., low crack-onset strain). Interestingly, the combination of A10 and the nonfused donor monomers (D7 and D8) produced ductile films with higher values of crack-onset strain than the other combinations. We attributed this effect to a possible change in solid-state morphologies and packing when the DPP (A10) acceptors were combined with dialkoxybenzene (D7) and bithiophene (D8).

2. Influence of Long and Branching Solubilizing Side Chains. As mentioned in the previous section, the effects of long and branching solubilizing side chains can dominate the mechanical properties of a polymer film. The tensile moduli of the films containing donor units with branching side chains, 2-hexyldecyl (D6, D7, and D9), were found to be lower than donor units with linear side chains. We also observed an increase in ductility of the films with either 2-hexyldecyl or 2-ethylhexyl side chains, namely, 14 out of 16 polymers in which the crack-onset strain exceeded 5% were found to be in this category. Interestingly, three of the most ductile polymers found in this study comprised the donor D7: A3D7 (crack-onset strain of 68%), A5D7 (57%), and A14D7 (14%). Significant differences between the acceptors A2 and A3, whose similar structures comprise of benzothiadiazole with two flanking thiophenes, were attributed to the locations of the alkyl side chains. For A2, the alkyl side chains ($C_{12}H_{25}$) are located on the two flanking thiophenes, whereas for A3, the alkyl side chains ($C_{14}H_{29}$) are connected to the benzothiadiazole via ether linkages. With the exception of A3D3, whose stiffness and ductility are on the same order as polymers with A2 in the backbone structure, all polymers comprising A3 are less stiff and more ductile than the A2 counterparts. Notably, A3D1 and A3D7 were found to withstand large tensile strains (~18% and ~68%, respectively).

The correlation between the structures of the side chains and the mechanical properties of the polymers could be explained in part from the solid-state molecular packing.[28] While the mechanical properties and the molecular packing or crystalline quality are not necessarily related in a straightforward manner, we can draw some qualitative insights from the effects of the side chains. For example, Yiu et al. demonstrated that branched side chains on a DPP-based polymer led to more steric hindrance between neighboring polymer chains and lower crystalline coherence length when compared to linear side chains.[29] Segalman and co-workers have shown that replacing the hexyl side chains on P3HT to 2-ethylhexyl side chains (P3EHT) reduced the melting temperature and the crystallization kinetics of the polymer.[30] Furthermore, the backbone of the adjacent P3EHT chains have been shown to be significantly tilted, resulting in the larger spacing between the chains and the lower intermolecular coupling.[31] These results suggest that there is a reduction in packing efficiency and lower crystallinity when branched side chains are introduced; these effects could potentially lead to increased deformability.

3. Notes and Unresolved Questions. As mentioned in the previous section, the ability to predict the mechanical responses of the D−A polymers will require not only knowledge of the molecular parameters (fused-ring and side chains) but also the propensity to form crystallites,[4] degree of crystallinity, and rigidity (i.e., glassy behavior) of the amorphous domains.[12] We noticed this limitation of the predictive nature of focusing on one aspect of the molecular structures as depicted in Figure 5a−d. Figure 5a and 5b rank the D−A polymers by the tensile moduli and the crack-onset strains while separating them into three groups: (1) fused rings in both donor and acceptor, (2) fused rings in the donor or in the acceptor, and (3) all isolated rings. Figure 5c and 5d separate the polymers by the nature of the solubilizing side chains: (1) only linear chains, (2) branching chains in either the donor or the acceptor, and (3) all branching side chains. Our initial hypotheses would suggest that the polymers with all isolated rings and with all branching chains would be the least stiff and the most ductile. While the general trends we described hold relatively well, we observed that the polymers in each group sample occupied a large range of both values of the mechanical properties and substantial overlap. We note that further studies are required to fully isolate the complicated interplay between the nature of the polymer backbone and the nature of the side chains and their effects on the mechanical properties. For example, poly(3-dodecylthiophene) has linear alkyl side chains and has been reported by us to have high crack-onset strains.[23] However, for D−A polymers with relatively higher rigidity in the backbone, the linear side chains are less likely to lead to high crack-onset strains. Furthermore, some polymers comprising both isolated rings and branching side chains performed poorly mechanically. We attributed such outliers to the unknown stiffness of the chains and the solid-state packing structures of the polymers.

In addition, the dispersity and molecular weight of the D−A polymers must also be taken into account when predicting the mechanical properties. For P3ATs, the dependencies of the solid-state packing structure on molecular weight and regioregularity have been previously reported.[32−35] Furthermore, Kim et al. reported significant changes in mechanical and optoelectrical properties of P3HT as a function of regioregularity.[5] These rigorously controlled experiments in which the molecular weight, dispersity, and regioregularity were isolated required carefully controlled synthesis that is only possible for very few polymers, such as P3ATs, which are produced by a quasi-living process.[5,36] For most D−A polymers that require a Stille polycondensation reaction, the control over the molecular weight and the dispersity of the product is typically not high.[36,37] Moreover, the size-exclusion chromatography (SEC) system used to measure the values of $Đ$ operates

DOI: 10.1021/acs.chemmater.6b00525
Chem. Mater. 2016, 28, 2363−2373

at low temperatures and employs chloroform as the solvent. In these conditions, aggregation of some polymers could lead to unrealistic $Đ$ values. Figure 5e–h plots the mechanical properties of the D–A polymers to the number-average molecular weight and $Đ$. We observed few correlations between the mechanical properties of the different D–A polymers and their molecular weight and $Đ$ (though the usual caveats apply of obtaining molecular weight for conjugated polymers by size-exclusion chromatography when no similarly rigid standards are available). It is noteworthy to point out that while comparing the effect of molecular weight and $Đ$ for a single polymer could potentially provide a meaningful trend, the molecular weight and dispersity of the polymer alone do not explain the measured differences in mechanical properties.

4. Introduction of an Electronic-Mechanical Merit Factor. We measured the mechanical properties of D–A polymers in the hope of identifying the design rules for optimizing the mechanical robustness and electrical properties for R2R fabrication. We observed that many of the D–A polymers tested exhibited brittle properties despite the low stiffness. This result suggests that it will be a significant challenge to incorporate some D–A polymers in applications demanding significant deformation as well as in R2R fabrication. However, we identified several promising candidates with favorable electronic and mechanical properties. We combined the power conversion efficiency as reported for the roll-fabricated solar cell reported in ref 8 and the tensile modulus and crack-onset strain into a new merit factor (ψ) defined as

$$\Psi = PCE \times \frac{1}{E_f} \times CoS \tag{1}$$

$$\Psi_{rel} = \Psi/\Psi_{P3HT} \tag{2}$$

where E_f is the tensile modulus and the CoS is the crack-onset strain. Figure 6 depicts the relative merit factor (Ψ_{rel}) of the polymers tested in this experiment when compared to the properties of P3HT. The blank cells represent the missing data (where at least one quantity was missing). Using this merit factor we identified nine promising polymers (highlighted in green), four of which comprise the donor D7. We note that the

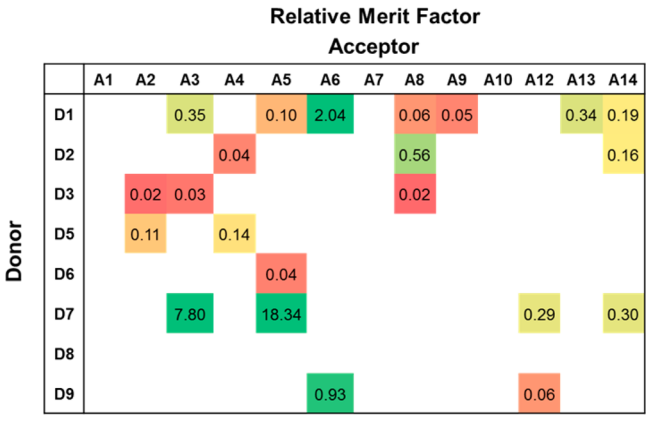

Figure 6. Relative merit factor incorporating the power conversion efficiency (PCE) as reported for the R2R fabricated solar cells (from ref 8), the tensile modulus, and crack-onset strains in relationship to those of P3HT. Blank cells indicate missing information where at least one quantity was missing. The tensile modulus of P3HT and crack-onset strain, reproduced from ref 23, were 1.09 ± 0.15 GPa and (9 ± 1.2)% respectively.

mechanical properties of the composites of the electron-donating polymer and an electron acceptor will be different than those of the pure polymers. The addition of fullerene-based electron acceptors (namely, [60] PCBM) has been reported by us and others to lower the mechanical robustness of the composites when compared to the pure polymers.[20,23] However, with the recent advancement in nonfullerene electron acceptors, this deleterious effect can potentially be avoided.[14] Furthermore, we admit to some shortcomings arising from the simplicity of the proposed figure of merit, namely, the equal contributions from power conversion efficiency, tensile modulus, and crack-onset strain. In order to characterize the electronic and mechanical properties fully, a more in-depth study of the effects of the addition of the electron acceptor, the film thickness, and the processing conditions on the electronic and mechanical properties of the whole modules will be required.

CONCLUSION

This paper described the mechanical properties of a library of D–A polymers with significant diversity in molecular structure. We identified some trends from the measured values of tensile modulus and crack-onset strain as well as plausible reasons for the exceptions. We found that the stiffness of most D–A polymers was on the same order of magnitude as P3HT or lower (occupying the range between 200 MPa to 1 GPa; however, most were brittle and tended to fracture at low strains, <5%). The polymers comprising the donors with fused rings tended to have higher stiffness and higher tendency to fracture. In addition, the polymers with branching solubilizing side chains were found to have high deformability. These trends are useful for general guidelines while designing highly mechanically robust materials for R2R fabrication. It is important to note the importance of co-optimization of electronic and mechanical properties for designing materials for both R2R fabrication and flexible or stretchable applications. From the library of D–A polymers, we identified potential candidates whose merit factors (weighted values comprising power conversion efficiency and mechanical properties) are better than those of P3HT. However, we also identified that the molecular structures of the D–A polymers do not completely govern the mechanical properties; further analysis of the solid-state packing structure from computation, microstructural analysis, and a complete theory thereof are required to fully understand the interplay between mechanical and electronic behaviors of this class of materials.

EXPERIMENTAL METHODS

Materials. Low-band-gap donor–acceptor polymers used for this work were described in a previous study by Bundgaard et al.[8] Briefly, 13 acceptor and 8 donor units (Figure 1a and 1b) were selected and all the combinations were synthesized, yielding 104 polymers. Several combinations were omitted in the mechanical studies due to difficulties in synthesis. After chemical and optoelectronic characterization of these materials, 75 polymers were initially available for mechanical characterizations. All of the polymers properties and synthesis procedures are reproduced from ref 8 in the Supporting Information. Polydimethylsiloxane (PDMS) (Sylgard 184) was purchased from Dow Corning. Chloroform and P3HT were purchased from Sigma-Aldrich and used as received.

Sample Preparation. The glass substrates (2.5 cm × 2.5 cm) were cleaned by bath sonication of Alconox solution, deionized water, acetone, and isopropanol for 10 min each and dried under compressed air before they were plasma treated for 3 min (30 W, 200 mTorr

DOI: 10.1021/acs.chemmater.6b00525
Chem. Mater. 2016, 28, 2363–2373

ambient air). All polymer solutions were prepared by dissolution in chloroform at a 20 mg mL^{-1} concentration. The solution was then stirred on a hot plate using a magnetic stirrer at 50 °C for 2 h before cooling to room temperature and filtering through a 1 μm glass microfiber filter. For each polymer, three different thicknesses were prepared by spin coating the solution on top of the plasma-treated glass substrates at 500, 1000, and 2000 rpm for 2.5 min.

Tensile Moduli and Crack-Onset Strains. Polydimethylsiloxane (PDMS) substrates were prepared according to the manufacturer's instruction at a ratio of 10:1 (base:cross-linker) and cured at room temperature for 36−48 h. PDMS strips (1 cm × 8 cm × 0.3 cm) were then cut out using a razor blade and stretched to strains of 4% using a computer-controlled stage (Newmark model ET-100-11) and clipped onto a glass substrate with binder clips. To transfer the polymer film onto the PDMS strip the previously spin-coated polymer film was then pressed onto the prestretched PDMS strip. The sample was then dipped into DI water for a time ranging from 30 s up to 20 min depending of the polymer. The sample was removed from the water with tweezers, and the glass substrate bearing the polymer was stripped of the PDMS, leaving the polymer layer on top of the PDMS. The sample was dried in a desiccator under dynamic vacuum for 30 min. Finally, the prestrained PDMS was released to form buckles. The buckled polymer films were observed with an optical microscope. Optical micrographs of the buckles were acquired and analyzed via an in-house MATLAB code. The tensile modulus of the PDMS was measured for each batch with a conventional pull tester, and the thickness of the each polymer film was measured using a Veeco Dektak stylus profilometer. The tensile modulus of the polymers was calculated using eq 3.

$$E_f = 3E_s\left(\frac{1-\nu_f^2}{1-\nu_s^2}\right)\left(\frac{\lambda_b}{2\pi d_f}\right)^3 \quad (3)$$

Briefly, the buckling wavelength λ_b was plotted as a function of the film thickness d_f. The slope λ_b/d_f obtained by linear fit was then substituted in eq 3, where E_s is the PDMS substrate modulus and the Poisson ratios of the film (ν_f) and the PDMS substrate (ν_s) were assumed to be 0.35 and 0.5 respectively.[20] We prepared our films to be within the range from ∼40 to 500 nm.[4,19,24,25] To minimize the change of experimental error, we also used the slope of the linear fit (λ_b/d_f) between the three data points. Ductility of the films as manifested in a form of the crack-onset strains were measured using the same film-on-elastomer method as described in previous work.[23] The polymer films transferred onto unstrained PDMS were then stretched using a computer-controlled linear actuator with a step size of 0.5% strain. Each step was imaged through an optical microscope to observe the generation of cracks. The crack-onset strain of each film was defined as the strain at which the first crack was observed.

■ ASSOCIATED CONTENT

Supporting Information

The Supporting Information is available free of charge on the ACS Publications website at DOI: 10.1021/acs.chemmater.6b00525.

Tables S1 and S2 and Figures S1 and S2, which relate spin-coating speed, film thickness, and mechanical properties (PDF)

■ AUTHOR INFORMATION

Corresponding Author

*E-mail: dlipomi@ucsd.edu.

Author Contributions

‡B.R. and S.S. contributed equally.

Notes

The authors declare no competing financial interest.

■ ACKNOWLEDGMENTS

This work was supported by the Eurotech Universities Alliance project "Interface science for photovoltaics (ISPV)" and by the Air Force Office of Scientific Research (AFOSR) Young Investigator Program, grant number FA9550-13-1-0156, awarded to D.J.L. This work was supported by the Villum Foundation's Young Investigator Programme (second round, project Materials for Energy Production) awarded to E.B. Additional support was provided by the National Science Foundation Graduate Research Fellowship under Grant No. DGE-1144086 and the Kaplan Dissertation Year Fellowship, awarded to S.S., and by laboratory startup funds from the University of California, San Diego.

■ REFERENCES

(1) Krebs, F. C.; Espinosa, N.; Hösel, M.; Søndergaard, R. R.; Jørgensen, M. 25th Anniversary Article: Rise to Power − OPV-Based Solar Parks. *Adv. Mater.* **2014**, *26*, 29−39.

(2) Savagatrup, S.; Printz, A. D.; O'Connor, T. F.; Zaretski, A. V.; Rodriquez, D.; Sawyer, E. J.; Rajan, K. M.; Acosta, R. I.; Root, S. E.; Lipomi, D. J. Mechanical Degradation and Stability of Organic Solar Cells: Molecular and Microstructural Determinants. *Energy Environ. Sci.* **2015**, *8*, 55−80.

(3) Bruner, C.; Miller, N. C.; McGehee, M. D.; Dauskardt, R. H. Molecular Intercalation and Cohesion of Organic Bulk Heterojunction Photovoltaic Devices. *Adv. Funct. Mater.* **2013**, *23*, 2863−2871.

(4) O'Connor, B.; Chan, E. P.; Chan, C.; Conrad, B. R.; Richter, L. J.; Kline, R. J.; Heeney, M.; McCulloch, I.; Soles, C. L.; DeLongchamp, D. M. Correlations between Mechanical and Electrical Properties of Polythiophenes. *ACS Nano* **2010**, *4*, 7538−7544.

(5) Kim, J.-S.; Kim, J.-H.; Lee, W.; Yu, H.; Kim, H. J.; Song, I.; Shin, M.; Oh, J. H.; Jeong, U.; Kim, T.-S.; et al. Tuning Mechanical and Optoelectrical Properties of Poly(3-Hexylthiophene) through Systematic Regioregularity Control. *Macromolecules* **2015**, *48*, 4339−4346.

(6) Printz, A. D.; Zaretski, A. V.; Savagatrup, S.; Chiang, A. S.-C.; Lipomi, D. J. Yield Point of Semiconducting Polymer Films on Stretchable Substrates Determined by Onset of Buckling. *ACS Appl. Mater. Interfaces* **2015**, *7*, 23257−23264.

(7) Dang, M. T.; Hirsch, L.; Wantz, G. P3HT:PCBM, Best Seller in Polymer Photovoltaic Research. *Adv. Mater.* **2011**, *23*, 3597−3602.

(8) Bundgaard, E.; Livi, F.; Hagemann, O.; Carlé, J. E.; Helgesen, M.; Heckler, I. M.; Zawacka, N. K.; Angmo, D.; Larsen-Olsen, T. T.; dos Reis Benatto, G. a.; et al. Matrix Organization and Merit Factor Evaluation as a Method to Address the Challenge of Finding a Polymer Material for Roll Coated Polymer Solar Cells. *Adv. Energy Mater.* **2015**, *5*, 1402186.

(9) Guo, X.; Baumgarten, M.; Müllen, K. Designing π-Conjugated Polymers for Organic Electronics. *Prog. Polym. Sci.* **2013**, *38*, 1832−1908.

(10) Liu, Y.; Zhao, J.; Li, Z.; Mu, C.; Ma, W.; Hu, H.; Jiang, K.; Lin, H.; Ade, H.; Yan, H. Aggregation and Morphology Control Enables Multiple Cases of High-Efficiency Polymer Solar Cells. *Nat. Commun.* **2014**, *5*, 5293.

(11) Lipomi, D. J.; Chong, H.; Vosgueritchian, M.; Mei, J.; Bao, Z. Toward Mechanically Robust and Intrinsically Stretchable Organic Solar Cells: Evolution of Photovoltaic Properties with Tensile Strain. *Sol. Energy Mater. Sol. Cells* **2012**, *107*, 355−365.

(12) Printz, A.; Savagatrup, S.; Burke, D.; Purdy, T.; Lipomi, D. Increased Elasticity of a Low-Bandgap Conjugated Copolymer by Random Segmentation for Mechanically Robust Solar Cells. *RSC Adv.* **2014**, *4*, 13635−13643.

(13) Wu, H.-C.; Benight, S. J.; Chortos, A.; Lee, W.-Y.; Mei, J.; To, J. W. F.; Lu, C.; He, M.; Tok, J. B.-H.; Chen, W.-C.; et al. A Rapid and Facile Soft Contact Lamination Method: Evaluation of Polymer Semiconductors for Stretchable Transistors. *Chem. Mater.* **2014**, *26*, 4544−4551.

DOI: 10.1021/acs.chemmater.6b00525
Chem. Mater. 2016, 28, 2363−2373

(14) Kim, T.; Kim, J.-H.; Kang, T. E.; Lee, C.; Kang, H.; Shin, M.; Wang, C.; Ma, B.; Jeong, U.; Kim, T.-S.; et al. Flexible, Highly Efficient All-Polymer Solar Cells. *Nat. Commun.* **2015**, *6*, 8547.
(15) Jackson, N. E.; Kohlstedt, K. L.; Savoie, B. M.; Olvera de la Cruz, M.; Schatz, G. C.; Chen, L. X.; Ratner, M. A. Conformational Order in Aggregates of Conjugated Polymers. *J. Am. Chem. Soc.* **2015**, *137*, 6254−6262.
(16) Duan, C.; Huang, F.; Cao, Y. Recent Development of Push−pull Conjugated Polymers for Bulk-Heterojunction Photovoltaics: Rational Design and Fine Tailoring of Molecular Structures. *J. Mater. Chem.* **2012**, *22*, 10416−10434.
(17) Takacs, C. J.; Brady, M. A.; Treat, N. D.; Kramer, E. J.; Chabinyc, M. L. Quadrites and Crossed-Chain Crystal Structures in Polymer Semiconductors. *Nano Lett.* **2014**, *14*, 3096−3101.
(18) Printz, A. D.; Savagatrup, S.; Rodriquez, D.; Lipomi, D. J. Role of Molecular Mixing on the Stiffness of Polymer:fullerene Bulk Heterojunction Films. *Sol. Energy Mater. Sol. Cells* **2015**, *134*, 64−72.
(19) Stafford, C. M.; Harrison, C.; Beers, K. L.; Karim, A.; Amis, E. J.; VanLandingham, M. R.; Kim, H.-C.; Volksen, W.; Miller, R. D.; Simonyi, E. E. A Buckling-Based Metrology for Measuring the Elastic Moduli of Polymeric Thin Films. *Nat. Mater.* **2004**, *3*, 545−550.
(20) Tahk, D.; Lee, H. H.; Khang, D.-Y. Elastic Moduli of Organic Electronic Materials by the Buckling Method. *Macromolecules* **2009**, *42*, 7079−7083.
(21) Awartani, O.; Lemanski, B. I.; Ro, H. W.; Richter, L. J.; DeLongchamp, D. M.; O'Connor, B. T. Correlating Stiffness, Ductility, and Morphology of Polymer:Fullerene Films for Solar Cell Applications. *Adv. Energy. Mater.* **2013**, *3*, 399−406.
(22) Dupont, S. R.; Oliver, M.; Krebs, F. C.; Dauskardt, R. H. Interlayer Adhesion in Roll-to-Roll Processed Flexible Inverted Polymer Solar Cells. *Sol. Energy Mater. Sol. Cells* **2012**, *97*, 171−175.
(23) Savagatrup, S.; Makaram, A. S.; Burke, D. J.; Lipomi, D. J. Mechanical Properties of Conjugated Polymers and Polymer-Fullerene Composites as a Function of Molecular Structure. *Adv. Funct. Mater.* **2014**, *24*, 1169−1181.
(24) Huang, H.; Chung, J. Y.; Nolte, A. J.; Stafford, C. M. Characterizing Polymer Brushes via Surface Wrinkling. *Chem. Mater.* **2007**, *19*, 6555−6560.
(25) Stafford, C. M.; Vogt, B. D.; Harrison, C.; Julthongpiput, D.; Huang, R. Elastic Moduli of Ultrathin Amorphous Polymer Films. *Macromolecules* **2006**, *39*, 5095−5099.
(26) Lee, J.-B.; Yoon, S.-S.; Khang, D.-Y. The Importance of Interfacial Adhesion in the Buckling-Based Mechanical Characterization of Materials. *RSC Adv.* **2013**, *3*, 17364−17372.
(27) Zhao, Y.; Zhao, X.; Zang, Y.; Di, C.; Diao, Y.; Mei, J. Conjugation-Break Spacers in Semiconducting Polymers: Impact on Polymer Processability and Charge Transport Properties. *Macromolecules* **2015**, *48*, 2048−2053.
(28) Mei, J.; Bao, Z. Side Chain Engineering in Solution-Processable Conjugated Polymers. *Chem. Mater.* **2014**, *26*, 604−615.
(29) Yiu, A. T.; Beaujuge, P. M.; Lee, O. P.; Woo, C. H.; Toney, M. F.; Fréchet, J. M. J. Side-Chain Tunability of Furan-Containing Low-Band-Gap Polymers Provides Control of Structural Order in Efficient Solar Cells. *J. Am. Chem. Soc.* **2012**, *134*, 2180−2185.
(30) Ho, V.; Boudouris, B. W.; Segalman, R. A. Tuning Polythiophene Crystallization through Systematic Side Chain Functionalization. *Macromolecules* **2010**, *43*, 7895−7899.
(31) Himmelberger, S.; Duong, D. T.; Northrup, J. E.; Rivnay, J.; Koch, F. P. V.; Beckingham, B. S.; Stingelin, N.; Segalman, R. a.; Mannsfeld, S. C. B.; Salleo, A. Role of Side-Chain Branching on Thin-Film Structure and Electronic Properties of Polythiophenes. *Adv. Funct. Mater.* **2015**, *25*, 2616−2624.
(32) Meille, S. V.; Romita, V.; Caronna, T.; Lovinger, A. J.; Catellani, M.; Belobrzeckaja, L. Influence of Molecular Weight and Regioregularity on the Polymorphic Behavior of Poly (3-Decylthiophenes). *Macromolecules* **1997**, *30*, 7898−7905.
(33) Goh, C.; Kline, R. J.; McGehee, M. D.; Kadnikova, E. N.; Fréchet, J. M. J. Molecular-Weight-Dependent Mobilities in Regioregular poly(3-Hexyl-Thiophene) Diodes. *Appl. Phys. Lett.* **2005**, *86*, 122110.
(34) Wu, Z.; Petzold, A.; Henze, T.; Thurn-Albrecht, T.; Lohwasser, R. H.; Sommer, M.; Thelakkat, M. Temperature and Molecular Weight Dependent Hierarchical Equilibrium Structures in Semiconducting Poly(3-Hexylthiophene). *Macromolecules* **2010**, *43*, 4646−4653.
(35) Kline, R. J.; McGehee, M. D.; Kadnikova, E. N.; Liu, J.; Frechet, J. M. J.; Toney, M. F. Dependence of Regioregular Poly (3-Hexylthiophene) Film Morphology and Field-Effect Mobility on Molecular Weight. *Macromolecules* **2005**, *38*, 3312−3319.
(36) Burke, D. J.; Lipomi, D. J. Green Chemistry for Organic Solar Cells. *Energy Environ. Sci.* **2013**, *6*, 2053−2066.
(37) Brouwer, F.; Alma, J.; Valkenier, H.; Voortman, T. P.; Hillebrand, J.; Chiechi, R. C.; Hummelen, J. C. Using Bis(pinacolato)-diboron to Improve the Quality of Regioregular Conjugated Co-Polymers. *J. Mater. Chem.* **2011**, *21*, 1582−1592.

DOI: 10.1021/acs.chemmater.6b00525
Chem. Mater. 2016, 28, 2363−2373